THE JOURNAL OF PHYSICAL CHEMISTRY C

Article

pubs.acs.org/JPCC

Structural and Electronic Properties of Pb- Intercalated Graphene on Ru(0001)

Xiangmin Fei, Lizhi Zhang, Wende Xiao,* Hui Chen, Yande Que, Liwei Liu, Kai Yang, Shixuan Du,* and Hong-Jun Gao

Institute of Physics, Chinese Academy of Sciences, Beijing 100190, China

Supporting Information

ABSTRACT: The Pb intercalation at the interface of monolayer graphene (MG) and Ru(0001) is studied by means of low temperature scanning tunneling microscopy (LT-STM) and Raman spectroscopy. Despite being covered by MG, the atomic structures of the Pb layer formed between MG and Ru(0001) have been directly imaged using LT-STM. The Pb layer intercalated underneath MG exhibits a $\sqrt{7} \times \sqrt{7}$-R19° superstructure with respect to the Ru(0001) surface. STM and Raman spectroscopy measurements and density functional theory calculations reveal that the epitaxial MG are effectively decoupled from the Ru(0001) substrate and recover its intrinsic electronic property after Pb intercalation.

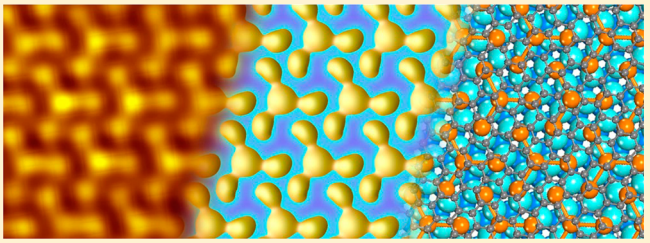

INTRODUCTION

As a single layer of sp^2-bonded carbon atoms with a honeycomb lattice, graphene has attracted considerable attention because of its unusual physical properties, such as the massless charge carriers and the quantum Hall effect.[1,2] Graphene is intrinsically nonsuperconductive.[3] Meanwhile, when a superconductor contacts with graphene, the coupling between the Cooper pairs and the relativistic massless Dirac Fermions may give rise to new quantum physics, for example, bipolar supercurrent and specular Andreev reflection.[4−7] Such graphene/superconductor heterostructures are very promising for developing novel devices with entirely new concepts.[3] It is highly desirable to "deposit" large-area and high-quality graphene with intrinsic electronic properties on superconductors.

In the past few years, the epitaxial growth of large-area uniform graphene with low defect density has been achieved on various transition metal substrates.[8−16] However, the electronic coupling between graphene and metal substrates may damage the characteristic Dirac cone band structure of graphene, which impedes many potential applications of epitaxial graphene.[17] For instance, high-quality single-crystalline monolayer graphene (MG) can be epitaxially grown on Ru(0001),[8−10] but its π band is strongly hybridized with the Ru 4d state,[18,19] resulting in a dramatic modification of the density of states (DOS) near the Fermi level and an n-doped feature of the thermoelectrical property.[11] In order to decouple the epitaxial graphene from the metal substrate and regain the intrinsic electronic properties of graphene, a buffer layer can be introduced at the interface of the graphene layer and its substrate. In recent years, it has been shown that intercalation of foreign materials, such as Pt,[20] Co,[20] and Si,[21−23] can efficiently weaken the interaction between MG and the Ru(0001) substrates, leading to the recovery of the intrinsic linear energy band dispersion of free-standing MG.[21] However, intercalation of a superconducting layer at the interface of MG and substrate and its impact on the electronic property of MG have been rarely addressed to date.[24] The atomic structures of the intercalated buffer layers are unclear, as they are covered by graphene, usually inaccessible for scanning tunneling microscopy (STM). Clarification of the atomic structure of the foreign materials intercalated at the interface of graphene and substrate remains a great challenge, but might be very helpful for tuning the electronic and transport properties of MG on metal substrate.

Previously, we investigated the growth and structural property of Pb on MG/Ru(0001).[25] In this work, we reported on the structural and electronic properties of Pb-intercalated MG on Ru(0001) by means of STM, scanning tunneling spectroscopy (STS) and Raman spectroscopy. Although the Pb atoms are covered by MG, we managed to obtain special tip states, so that the MG seems to be transparent, allowing direct imaging the atomic structures of Pb layer intercalated between graphene and Ru(0001) by STM. The Pb atoms intercalated underneath MG form a close-packed layer exhibiting a $\sqrt{7} \times \sqrt{7}$-R19° superstructure with respect to the Ru(0001) surface, which can effectively decouple MG from Ru(0001) and restore the intrinsic electronic property of MG, as revealed by STM/STS and Raman spectroscopy measurements and density functional theory (DFT) calculations.

Received: January 18, 2015
Revised: March 16, 2015
Published: March 20, 2015

DOI: 10.1021/acs.jpcc.5b00528
J. Phys. Chem. C 2015, 119, 9839−9844

EXPERIMENTAL SECTION

Our experiments were carried out in an ultrahigh vacuum (base pressure of 1×10^{-10} mbar) low temperature (LT) STM system (Unisoku), equipped with standard surface preparation facilities. The Ru(0001) (Mateck, Germany) surface was prepared by repeated cycles of Ar^+ sputtering and annealing at 950 °C. High-quality and large-area MG was obtained via pyrolysis of ethylene on Ru(0001), as described elsewhere.[9,11,25] Pb was deposited via vacuum sublimation from a homemade Knudsen-type evaporator at ∼200 °C, while the MG/Ru(0001) substrate were held at room temperature (RT). The Pb source was thoroughly degassed prior to Pb deposition. The typical deposition rate was ∼0.01 monolayer (ML)/min (1 ML = 9.4×10^{14} atoms/cm^2, corresponding to a single layer of bulk Pb(111)), as calibrated by LT-STM. The intercalation of the Pb atoms underneath graphene was achieved by sample annealing to appropriate temperature. STM images were acquired in constant-current mode, and all given voltages refer to the sample. Differential conductance (dI/dV) spectra were collected by using a lock-in technique with a 5 mV_{rms} sinusoidal modulation at a frequency of 973 Hz. All STM/STS experiments were performed with electrochemically etched tungsten tips at 4.2 K. Raman spectra were acquired by a Renishaw spectrometer at 532 nm with 1 mW power.

All DFT calculations were performed with the Vienna Ab Initio Simulation Package (VASP) and the projector augmented wave (PAW) method.[26,27] Local density approximation (LDA) in the form of Perdew−Zunger was adopted for the exchange-correlation functional.[28,29] The energy cutoff of the plane-wave basis sets is 400 eV. The periodic slab models of the metal substrate include four Ru layers and a vacuum layer with a thickness of 15 Å. In geometric optimizations, the bottom Ru layer was fixed, while the other Ru layers, Pb atoms and graphene were fully relaxed, until the residual forces were smaller than 0.02 eV/Å. For the 8 × 7 model, a mesh of 3 × 3 × 1 k-points sampling was used for the STM image simulation. When calculating the band structure of the $\sqrt{7} \times \sqrt{7}$-R19° model, the *k*-points sampling was 9 × 9 × 1 (see Supporting Information).

RESULTS AND DISCUSSION

The as-prepared MG on Ru(0001) shows a regular moiré pattern with a periodicity of ∼3 nm (Figure 1a) due to the lattice mismatch between MG and Ru(0001) surface.[9−11] Each unit cell of this moiré pattern includes three different regions, namely, atop, fcc, and hcp regions. The carbon atoms of the atop regions of the bottom layer graphene are seated on top of the ruthenium atoms of Ru(0001) substrate, while those of the fcc and hcp regions are stacked at the fcc and hcp hollow sites of the substrate, respectively.[9−11] The inhomogeneous interaction between MG and Ru(0001) substrate results in the geometrical corrugation of MG and different local electronic structures of the atop, fcc, and hcp regions,[18,19,30−32] which can dramatically influence the growth and structure of organic molecules and metals.[31,33−36]

Thermal evaporation of ∼0.5 ML Pb on MG/Ru(0001) at RT results in the formation of flat (111)-faceted Pb islands with lateral sizes in the range of a few tens to one hundred nanometers and heights of several nanometers.[25] After sample annealing to ∼300 °C for 1 h, no Pb island can be found in STM images. The moiré pattern of MG is significantly distorted and only preserved as small patches, which are surrounded by

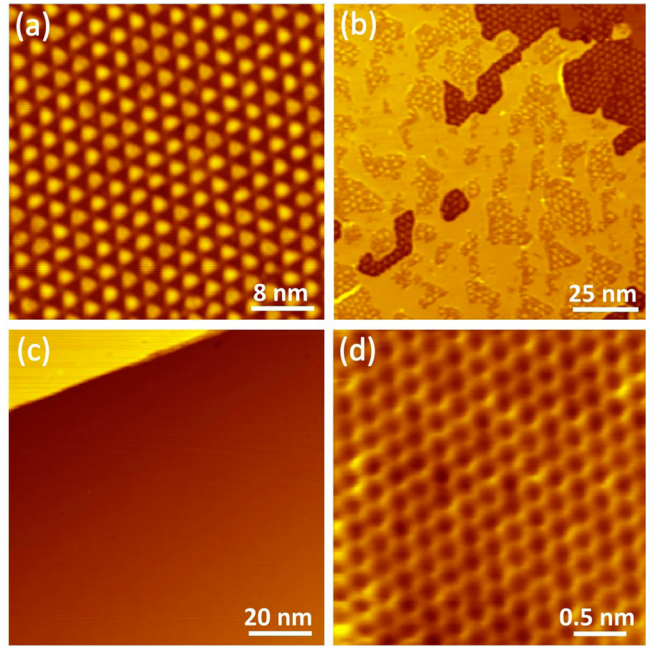

Figure 1. STM images of MG before and after Pb intercalation. (a) MG grown on Ru(0001) showing moiré pattern with a periodicity of ∼3 nm (sample bias, $U = -200$ mV; tunneling current, $I = 13$ pA). (b) After sample annealing at ∼300 °C for 1 h, the Pb atoms are intercalated between MG and Ru(0001) ($U = -1.5$ V, $I = 9.6$ pA). Note that the step edges become very irregular and two features, flat and corrugated areas, can be observed on the terraces. (c) After sample annealing at ∼400 °C for 1 h, the step edges become straight again ($U = -200$ mV, $I = 13$ pA). (d) Honeycomb lattice of MG after Pb intercalation ($U = -132$ mV, $I = 37$ pA).

flat areas with a roughness of ∼0.1 Å, as shown in Figure 1b. Moreover, the step edges become very irregular after sample annealing, in contrast to the straight step edges of MG/Ru(0001). After Pb deposition of ∼1 ML and subsequent sample annealing to ∼400 °C for 1 h, we observe the formation of extended flat terraces. The step edges become straight again, as seen in Figure 1c. These behaviors indicate that the Pb atoms have been intercalated underneath MG and could dramatically alter the shape of step edges of Ru(0001). Figure 1d shows a high-resolution STM image on a flat terrace. A perfect honeycomb lattice with a lattice constant of 2.46 ± 0.02 Å is revealed, well consistent with that of free-standing MG. We note that for MG grown on Ru(0001) the symmetry between the A- and B-sublattices (AB-symmetry) in the atop regions is essentially preserved, as the carbon atoms in these regions are located on top of the ruthenium atoms and the C−Ru coupling is very weak. Meanwhile, the AB-symmetry of MG is broken in the fcc and hcp regions,[18,19] as the carbon atoms of the A- and B-sublattices are stacked at different sites with respect to the substrate. Thus, honeycomb lattices can usually be resolved by STM measurements in the atop regions, corresponding to two sublattices, whereas only hexagonal lattices can be resolved in the fcc and hcp regions,[8−10] corresponding to one of the sublattices. Therefore, the observation of honeycomb lattice and the disappearance of the moiré pattern of MG indicate the decoupling of MG and Ru(0001) by the Pb intercalation, which results in nearly free-standing MG. Recently, Jin and co-workers studied the intercalation of Pb at MG/Ru(0001) interfaces by means of low energy electron microscopy and photoemission electron microscopy,[24] and reported that the Pb intercalation

DOI: 10.1021/acs.jpcc.5b00528
J. Phys. Chem. C 2015, 119, 9839−9844

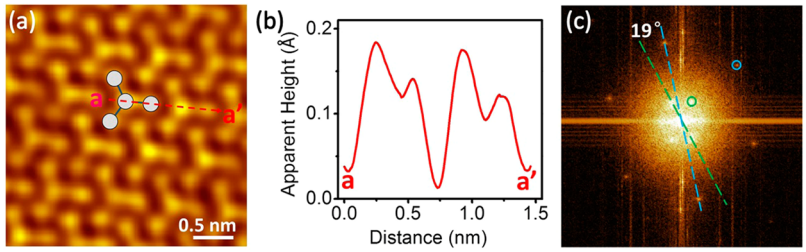

Figure 2. (a) STM image acquired on MG after Pb intercalation with special tip states showing the atomic structure of intercalated Pb flat layer (U = −200 mV, I = 13 pA). (b) Line profile along the red dashed line shown in (a). (c) FFT pattern of a large-scale STM image where the zoom-in shown in (a) is collected. The outer set of spots correspond to the reciprocal lattice of the intercalated Pb layer, while the inner set of spots are assigned to that of the MG moiré pattern.

decouples MG from the substrate and thus removes the superstructure of MG, in line with our results. Our STM measurements show that the defect density of MG after Pb intercalation is essentially similar to that before Pb intercalation, suggesting that Pb intercalation exerts no significant effect on the quality of MG. Similar behavior has been observed for the intercalation of Pd, Pt, Ni, Co, and Si at the interface of MG and Ru(0001).[20] Thus, we propose that the Pb intercalation may follow the similar mechanism as Pd does,[20] involving metal atom aided defect and self-healing of C−C bonds at high temperature.

It is well-known that STM is very sensitive to the surface structure and its depth sensitivity, that is, its ability to image substructure, is largely hindered due to the screening of the surface layer. Atomic resolution STM images of ordered lattices buried under surfaces were only reported in a few systems.[37,38] As the Pb atoms are intercalated underneath MG, it is difficult to resolve the atomic structure of the Pb layer by STM. Nevertheless, we manage to obtain special tip states, so that the MG covered Pb atoms seems to be transparent, allowing direct imaging the atomic structure of the intercalated Pb in real space. It has been demonstrated that a tip modified by CO or organic molecules can significantly improve the spatial resolution of STM.[39,40] Although the detailed structure of the tip is not clear, we believe that the tungsten tip might have been modified by some Pb atoms or residual gas molecules in the ultrahigh vacuum chamber, leading to the insensitivity of MG during STM measurements and reproducible imaging of Pb atoms covered by MG. Figure 2a shows a high-resolution STM image on the flat area with such a special tip state. It is seen that the intercalated Pb atoms form a hexagonal lattice. Each unit cell consists of a 3-fold symmetric "Y"-shaped tetramer. Line profile analysis (Figure 2b) reveals a periodicity of ∼7 Å for the hexagonal lattice of the Pb tetramers, twice of the lattice constant of the Pb(111) surface, whereas a separation of ∼3 Å is measured between the central Pb atom and the other ones of a tetramer. Therefore, the intercalated Pb layer can be viewed as a 2 × 2 superstructure with respect to the Pb(111) surface but with a similar atom density.

The structure of the intercalated layer with respect to MG and Ru(0001) can be extracted from the fast Fourier transformation (FFT) analysis of the STM images. Figure 2c illustrates the FFT pattern of a large-scale STM image where the zoom-in shown in Figure 2a is collected. Two sets of spots can be identified, as indicated by the blue and green circles. The outer set of spots correspond to the reciprocal lattice of the intercalated Pb layer, while the inner set of spots are assigned to that of the MG moiré pattern. A rotation angle of ∼19° between the two sets of dots is evaluated. Previous experiments and theoretical calculations revealed that the lattice vectors of the Ru(0001) substrate are parallel to that of MG moiré pattern.[8,9,18,19] Thus, the lattice vectors of the intercalated Pb layer are rotated by ∼19° with respect to the Ru(0001) surface. As the lattice length of the intercalated Pb layer is ∼7 Å, about $\sqrt{7}$ times of the lattice constant of 2.68 Å for Ru(0001) surface, we conclude that the intercalated Pb layer can be described as a $\sqrt{7} \times \sqrt{7}$-R19° superstructure with respect to the Ru(0001) surface. For a "Y"-shaped tetramer, the distance between the central Pb atom and the other three ones is ∼3 Å, significantly shorter than the lattice constant of ∼3.5 Å for the Pb(111) surface. Recently, Yuhara and co-workers studied the growth of Pb on Ru(0001) by low energy electron diffraction and STM, and found that Pb forms a similar $\sqrt{7} \times \sqrt{7}$-R19° superstructure with respect to the Ru(0001) surface.[41] However, the Pb films show close-packed hexagonal lattice with a lattice constant of 3.5 Å, which can be viewed as a 1 × 1 structure with respect to the Pb(111) surface.[41] Thus, the formation of "Y"-shaped tetramers after Pb intercalated at the interface of MG and Ru(0001) is probably due to the interaction between MG and Pb.

The structural and electronic properties Pb layer intercalated MG on Ru(0001) are also studied by DFT calculations. According to the experimental observations, the Pb layer intercalated MG on Ru(0001) is described by a model with 8 × 8 carbon atoms sitting on 7 × 7 ruthenium atoms with 7 "Y"-shaped Pb tetramers between the carbon and ruthenium atoms (8 × 7 model). Figure 3a shows the top view of the optimized structural model of Pb layer intercalated MG on Ru(0001). The simulated STM image shown in Figure 3b reproduces the STM images very well. Our DFT calculations reveal that the central Pb atoms of the "Y"-shaped tetramers are located at the fcc hollow sites of the Ru(0001) surface. After Pb layer intercalation the corrugated moiré pattern of MG/Ru(0001) disappears and the MG becomes very flat. The Pb−Ru separation is in the range of 2.38∼2.46 Å (Figure 3c), suggesting a strong coupling between Pb layer and Ru(0001) substrate. Meanwhile, the distance between MG and Pb layer is in the range of 3.63∼3.70 Å (Figure 3c), much longer than the calculated Ru−C separation of ∼2.2 Å for the fcc and hcp regions of MG/Ru(0001), but very similar to that of the atop regions.[18,19] It is known that the interaction between MG and Ru is very strong for the fcc and atop regions, while the MG is nearly free-standing for the atop regions.[18,19] Thus, the coupling between MG and Pb layer is very weak, leading to the recovery of the intrinsic electronic properties of MG. As the 8 × 7 model described above is too large to calculate the band structure in a reasonable time, we use a smaller model that can be described as the $\sqrt{7} \times \sqrt{7}$-R19° superstructure with respect

DOI: 10.1021/acs.jpcc.5b00528
J. Phys. Chem. C 2015, 119, 9839−9844

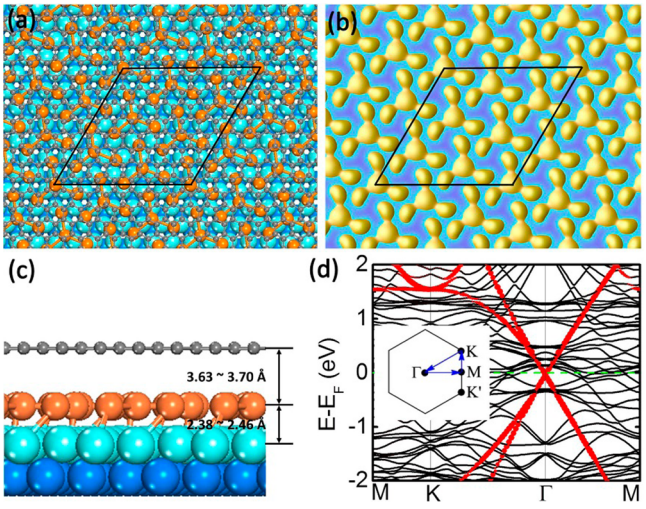

Figure 3. (a) Top view of the optimized structural model (8 × 7 model) of Pb layer intercalated MG on Ru(0001). The central Pb atoms of the "Y"-shaped tetramers are located at the fcc hollow sites of the Ru(0001) surface. The unit cell is indicated by the black rhombus. (b) Simulated STM image of MG/Pb/Ru(0001). (c) Lateral view showing that the Pb−Ru separation is in the range of 2.38~2.46 Å, while the distance between MG and Pb layer is in the range of 3.63~3.70 Å. (d) Calculated band structure of the Pb layer intercalated MG on Ru(0001) using the $\sqrt{7} \times \sqrt{7}$-R19° model. The red dots are projected DOS of C p_z state, showing a linear dispersion around Γ-point of graphene.

to the Ru(0001) surface ($\sqrt{7} \times \sqrt{7}$-R19° model, see Supporting Information). After structural optimization of this model, the Pb−Ru and Ru−C separations are 2.42 and 3.65 Å, respectively, similar to the ones obtained using the 8 × 7 model. Moreover, both models exhibit similar density of states. These behaviors indicate that the $\sqrt{7} \times \sqrt{7}$-R19° model is nearly equivalent to the 8 × 7 one for studying the electronic structures of the Pb layer intercalated MG on Ru(0001). Figure 3d shows the calculated band structure of the Pb layer intercalated MG on Ru(0001) using the $\sqrt{7} \times \sqrt{7}$-R19° model. A linear dispersion around Γ-point is clearly seen, in line with the experimental observations that MG recovers the intrinsic electronic property after intercalation of Pb layer.

The recovery of intrinsic electronic property of MG after Pb intercalation is experimentally confirmed by STS and Raman spectroscopy measurements. Figure 4a shows a typical dI/dV spectrum of Pb-intercalated MG on Ru(0001). A "V"-shaped DOS around Fermi level is clearly seen. Similar spectra are

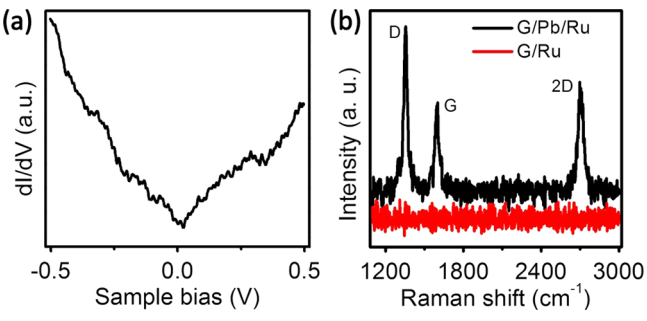

Figure 4. (a) dI/dV spectrum acquired on Pb intercalated MG on Ru(0001). (b) Raman spectra of MG/Ru(0001) before (red) and after (black) Pb intercalation.

acquired on different sites of MG/Pb/Ru(0001) unit cells. These behaviors differ from the site-dependent DOS in a unit cell of MG/Ru(0001) moiré pattern revealed by previous STM/STS experiments and DFT calculations,[9,18,42,43] indicating that the intercalated Pb layer decouples the MG from the Ru(0001) substrate and restores the free-standing feature of MG. Figure 4b shows the Raman spectra acquired on the MG/Ru(0001) sample before and after Pb intercalation. Prior to Pb intercalation, the Raman spectrum of MG/Ru(0001) is essentially featureless (the red line), due to the hybridization of the π-electrons of graphene and the Ru 4d state.[18,19] In contrast, the characteristic Raman spectrum of free-standing MG, including the G and 2D peaks, is collected after Pb intercalation (the black line), again indicating that the intercalated Pb layer at the MG/Ru(0001) interface effectively weakens the coupling between the MG and the metal substrate and recovers the intrinsic electronic properties of MG. The D peak in the Raman spectrum indicates the presence of graphene edges, which might be due to a Pb coverage of less than 1 ML.

CONCLUSIONS

We have studied the structural and electronic properties of Pb intercalated MG on Ru(0001) by means of LT-STM and Raman spectroscopy. Although the Pb atoms are covered by MG, we manage to obtain special tip states, so that the MG seems to be transparent, allowing direct imaging the atomic structures of Pb layer intercalated between graphene and Ru(0001) by LT-STM. We find that the intercalated Pb layer exhibits a $\sqrt{7} \times \sqrt{7}$-R19° superstructure with respect to the Ru(0001) surface. STM/STS and Raman spectroscopy measurements and DFT calculations reveal that the epitaxial MG are effectively decoupled from the Ru(0001) substrate, resulting in the flattening (disappearance of moiré pattern) and recovery of intrinsic electronic property of MG. Our work constitutes an important step to fabricate a graphene/superconductor/metal heterostructure. Intercalation of thick Pb layer underneath graphene is under the way, which is expected to have wide application in microelectronics-oriented devices based on high quality graphene.

ASSOCIATED CONTENT

Supporting Information

Two structural models of Pb layer intercalated MG on Ru(0001) used in DFT calculations. This material is available free of charge via the Internet at http://pubs.acs.org.

AUTHOR INFORMATION

Corresponding Authors

*Tel.: +86-10-82648035. Fax: +86-10-62556598. E-mail: wdxiao@iphy.ac.cn.
*E-mail: sxdu@iphy.ac.cn.

Notes

The authors declare no competing financial interest.

ACKNOWLEDGMENTS

We would like to gratefully acknowledge financial support from MOST (Nos. 2011CB932700 and 2010CB 923004), NSFC (Nos. 51325204 and 61390501), Shanghai Supercomputer Center, and CAS in China.

DOI: 10.1021/acs.jpcc.5b00528
J. Phys. Chem. C 2015, 119, 9839−9844

REFERENCES

(1) Novoselov, K. S.; Geim, A. K.; Morozov, S. V.; Jiang, D.; Katsnelson, M. I.; Grigorieva, I. V.; Dubonos, S. V.; Firsov, A. A. Two-Dimensional Gas of Massless Dirac Fermions in Graphene. *Nature* **2005**, *438*, 197−200.

(2) Zhang, Y.; Tan, Y.-W.; Stormer, H. L.; Kim, P. Experimental Observation of the Quantum Hall Effect and Berry's Phase in Graphene. *Nature* **2005**, *438*, 201−204.

(3) Beenakker, C.W. J. Colloquium: Andreev Reflection and Klein Tunneling in Graphene. *Rev. Mod. Phys.* **2008**, *80*, 1337−1354.

(4) Heersche, H. B.; Jarillo-Herrero, P.; Oostinga, J. B.; Vandersypen, L. M. K.; Morpurgo, A. F. Bipolar Supercurrent in Graphene. *Nature* **2007**, *446*, 56−59.

(5) Beenakker, C. W. J. Specular Andreev Reflection in Graphene. *Phys. Rev. Lett.* **2006**, *97*, 067007.

(6) Miao, F.; Wijeratne, S.; Zhang, Y.; Coskun, U. C.; Bao, W.; Lau, C. N. Phase-Coherent Transport in Graphene Quantum Billiards. *Science* **2007**, *317*, 1530−1533.

(7) Dirks, T.; Hughes, T. L.; Lal, S.; Uchoa, B.; Chen, Y.-F.; Chialvo, C.; Goldbart, P. M.; Mason, N. Transport through Andreev Bound States in a Graphene Quantum Dot. *Nat. Phys.* **2011**, *7*, 386−390.

(8) Pan, Y.; Shi, D.-X.; Gao, H.-J. Formation of Graphene on Ru(0001) Surface. *Chin. Phys. (Beijing, China)* **2007**, *16*, 3151−3153.

(9) Pan, Y.; Zhang, H.; Shi, D.; Sun, J.; Du, S.; Liu, F.; Gao, H.-J. Highly Ordered, Millimeter-Scale, Continuous, Single-Crystalline Graphene Monolayer Formed on Ru (0001). *Adv. Mater.* **2009**, *21*, 2777−2780.

(10) Sutter, P. W.; Flege, J.-I.; Sutter, E. A. Epitaxial Graphene on Ruthenium. *Nat. Mater.* **2008**, *7*, 406−411.

(11) Gao, M.; Pan, Y.; Zhang, C. D.; Hu, H.; Yang, R.; Lu, H. L.; Cai, J. M.; Du, S. X.; Liu, F.; Gao, H.-J. Tunable Interfacial Properties of Epitaxial Graphene on Metal Substrates. *Appl. Phys. Lett.* **2010**, *96*, 053109.

(12) Li, X. S.; Cai, W. W.; An, J. H.; Kim, S.; Nah, J.; Yang, D. X.; Piner, R.; Velamakanni, A.; Jung, I.; Tutuc, E.; et al. Large-Area Synthesis of High-Quality and Uniform Graphene Films on Copper Foils. *Science* **2009**, *324*, 1312−1314.

(13) Ugeda, M. M.; Fernández-Torre, D.; Brihuega, I.; Pou, P.; Martínez-Galera, A. J.; Pérez, R.; Gómez-Rodríguez, J. M. Point Defects on Graphene on Metals. *Phys. Rev. Lett.* **2011**, *107*, 116803.

(14) Gao, M.; Pan, Y.; Huang, L.; Hu, H.; Zhang, L. Z.; Guo, H. M.; Du, S. X.; Gao, H.-J. Epitaxial Growth and Structural Property of Graphene on Pt(111). *Appl. Phys. Lett.* **2011**, *98*, 033101.

(15) N'Diaye, A. T.; Bleikamp, S.; Feibelman, P. J.; Michely, T. Two-Dimensional Ir Cluster Lattice on a Graphene Moiré on Ir(111). *Phys. Rev. Lett.* **2006**, *97*, 215501.

(16) Wintterlin, J.; Bocquet, M. L. Graphene on Metal Surfaces. *Surf. Sci.* **2009**, *603*, 1841−1852.

(17) Voloshina, E.; Dedkov, Y. Graphene on Metallic Surfaces: Problems and Perspectives. *Phys. Chem. Chem. Phys.* **2012**, *14*, 13502−13514.

(18) Wang, B.; Bocquet, M.-L.; Marchini, S.; Günther, S.; Wintterlin, J. Chemical Origin of a Graphene Moiré Overlayer on Ru(0001). *Phys. Chem. Chem. Phys.* **2008**, *10*, 3530−3534.

(19) Jiang, D.-E.; Du, M.-H.; Dai, S. First Principles Study of the Graphene/Ru(0001) Interface. *J. Chem. Phys.* **2009**, *130*, 074705.

(20) Huang, L.; Pan, Y.; Pan, L.; Gao, M.; Xu, W.; Que, Y.; Zhou, H.; Wang, Y.; Du, S.; Gao, H. J. Intercalation of Metal Islands and Films at the Interface of Epitaxially Grown Graphene and Ru(0001) Surfaces. *Appl. Phys. Lett.* **2011**, *99*, 163107.

(21) Mao, J.; Huang, L.; Pan, Y.; Gao, M.; He, J.; Zhou, H.; Guo, H.; Tian, Y.; Zou, Q.; Zhang, L.; et al. Silicon Layer Intercalation of Centimeter-Scale, Epitaxially Grown Monolayer Graphene on Ru(0001). *Appl. Phys. Lett.* **2012**, *100*, 093101.

(22) Cui, Y.; Gao, J.; Jin, L.; Zhao, J.; Tan, D.; Fu, Q.; Bao, X. An Exchange Intercalation Mechanism for the Formation of a Two-dimensional Si Structure underneath Graphene. *Nano Res.* **2012**, *5*, 352−360.

(23) Lizzit, S.; Larciprete, R.; Lacovig, P.; Dalmiglio, M.; Orlando, F.; Baraldi, A.; Gammelgaard, L.; Barreto, L.; Bianchi, M.; Perkins, E.; et al. Transfer-Free Electrical Insulation of Epitaxial Graphene from Its Metal Substrate. *Nano Lett.* **2012**, *12*, 4503−4507.

(24) Jin, L.; Fu, Q.; Mu, R.; Tan, D.; Bao, X. Pb Intercalation underneath a Graphene Layer on Ru(0001) and Its Effect on Graphene Oxidation. *Phys. Chem. Chem. Phys.* **2011**, *13*, 16655−16660.

(25) Liu, L. W.; Xiao, W. D.; Yang, K.; Zhang, L. Z.; Jiang, Y. H.; Fei, X. M.; Du, S. X.; Gao, H. J. Growth and Structural Properties of Pb Islands on Epitaxial Graphene on Ru(0001). *J. Phys. Chem. C* **2013**, *117*, 22652−22655.

(26) Vanderbilt, D. Soft Self-Consistent Pseudopotentials in a Generalized Eigenvalue Formalism. *Phys. Rev. B* **1990**, *41*, 7892−7895.

(27) Kresse, G.; Furthmüller, J. Efficient Iterative Schemes for Ab Initio Total-Energy Calculations using a Plane-Wave Basis Set. *Phys. Rev. B* **1996**, *54*, 11169−11186.

(28) Ceperley, D. M.; Alder, B. J. Ground State of the Electron Gas by a Stochastic Method. *Phys. Rev. Lett.* **1980**, *45*, 566−569.

(29) Perdew, J. P.; Zunger, A. Self-Interaction Correction to Density-Functional Approximations for Many-Electron Systems. *Phys. Rev. B* **1981**, *23*, 5048−5079.

(30) Zhang, H. G.; Hu, H.; Pan, Y.; Mao, J. H.; Gao, M.; Guo, H. M.; Du, S. X.; Greber, T.; Gao, H.-J. Graphene Based Quantum Dots. *J. Phys.: Condens. Matter* **2010**, *22*, 302001.

(31) Zhang, H. G.; Sun, J. T.; Low, T.; Zhang, L. Z.; Pan, Y.; Liu, Q.; Mao, J. H.; Zhou, H. T.; Guo, H. M.; Du, S. X.; et al. Assembly of Iron Phthalocyanine and Pentacene Molecules on a Graphene Monolayer Grown on Ru(0001). *Phys. Rev. B* **2011**, *84*, 245436.

(32) Feng, W.; Lei, S. L.; Li, Q. X.; Zhao, A. D. Periodically Modulated Electronic Properties of the Epitaxial Monolayer Graphene on Ru(0001). *J. Phys. Chem. C* **2011**, *115*, 24858−24864.

(33) Zhang, H. G.; Xiao, W. D.; Mao, J. H.; Zhou, H. T.; Li, G.; Zhang, Y.; Liu, L. W.; Du, S. X.; Gao, H.-J. Host−Guest Superstructures on Graphene-Based Kagome Lattice. *J. Phys. Chem. C* **2012**, *116*, 11091−11095.

(34) Yang, K.; Xiao, W. D.; Jiang, Y. H.; Zhang, H. G.; Liu, L. W.; Mao, J. H.; Zhou, H. T.; Du, S. X.; Gao, H.-J. Molecule−Substrate Coupling between Metal Phthalocyanines and Epitaxial Graphene Grown on Ru(0001) and Pt(111). *J. Phys. Chem. C* **2012**, *116*, 14052−14056.

(35) Mao, J.; Zhang, H.; Jiang, Y.; Pan, Y.; Gao, M.; Xiao, W.; Gao, H. J. Tunability of Supramolecular Kagome Lattices of Magnetic Phthalocyanines Using Graphene-Based Moiré Patterns as Templates. *J. Am. Chem. Soc.* **2009**, *131*, 14136−14137.

(36) Pan, Y.; Gao, M.; Huang, L.; Liu, F.; Gao, H.-J. Directed Self-assembly of Monodispersed Platinum Nanoclusters on Graphene Moiré Template. *Appl. Phys. Lett.* **2009**, *95*, 093106.

(37) Altfeder, I. B.; Chen, D. M.; Matveev, K. A. Imaging Buried Interfacial Lattices with Quantized Electrons. *Phys. Rev. Lett.* **1998**, *80*, 4895−4898.

(38) Rogero, C.; Martín-Gago, J. A.; Cerdá, J. I. Subsurface Structure of Epitaxial Rare-Earth Silicides Imaged by STM. *Phys. Rev. B* **2006**, *74*, 121404(R).

(39) Deng, Z. T.; Lin, H.; Ji, W.; Gao, L.; Lin, X.; Cheng, Z. H.; He, X. B.; Lu, J. L.; Shi, D. X.; Hofer, W. A.; et al. Selective Analysis of Molecular States by Functionalized Scanning Tunneling Microscopy Tips. *Phys. Rev. Lett.* **2006**, *96*, 156102.

(40) Repp, J.; Meyer, G.; Paavilainen, S.; Olsson, F. E.; Persson, M. Scanning Tunneling Spectroscopy of Cl Vacancies in NaCl Films: Strong Electron-Phonon Coupling in Double-Barrier Tunneling Junctions. *Phys. Rev. Lett.* **2005**, *95*, 225503.

(41) Yuhara, J.; Ishikawa, Y.; Matsui, T. Two-Dimensional Alloy of Immiscible Pb and Sn Atoms on Ru(0001). *Surf. Sci.* **2013**, *616*, 131−136.

(42) Marchini, S.; Günther, S.; Wintterlin, J. Scanning Tunneling Microscopy of Graphene on Ru(0001). *Phys. Rev. B* **2007**, *76*, 075429.

(43) Vázquez de Parga, A. L.; Calleja, F.; Borca, B.; Passeggi, M. C. G.; Hinarejos, J. J.; Guinea, F.; Miranda, R. Periodically Rippled

DOI: 10.1021/acs.jpcc.5b00528
J. Phys. Chem. C 2015, 119, 9839−9844

Graphene: Growth and Spatially Resolved Electronic Structure. *Phys. Rev. Lett.* **2008**, *100*, 056807.

DOI: 10.1021/acs.jpcc.5b00528
J. Phys. Chem. C 2015, 119, 9839−9844